NUCL SCI TECH (2017) 28:117
DOI 10.1007/s41365-017-0258-z

Two-stage EEHG for coherent hard X-ray generation based on a superconducting linac

Zhen-Tang Zhao[1] · Chao Feng[1] · Kai-Qing Zhang[1]

Received: 11 June 2017 / Revised: 13 June 2017 / Accepted: 14 June 2017 / Published online: 10 July 2017

Abstract A two-stage echo-enabled harmonic generation (EEHG) scheme is proposed for a superconducting linac-driven FEL to produce coherent hard X-rays. Electron beams of quite different bunch lengths are separately used in each stage of EEHG, and a monochromator is designed to purify the radiation from the first stage for seeding the second stage. Theoretical analysis and 3D simulations indicate that the proposed scheme can generate high-repetition-rate coherent hard X-ray pulses directly from a conventional UV seed laser.

Keywords EEHG · Fresh beam · X-ray monochromator · Superconducting accelerator

1 Introduction

Free-electron laser (FEL) is considered as the fourth-generation light source as it is capable of producing extremely high-intensity, coherent, and ultra-short radiation pulses, which can open up new frontiers of ultra-fast and ultra-small sciences at the atomic scale. In X-ray wavelengths, most of the existing FEL facilities [1–6] are based on the self-amplified spontaneous emission (SASE) principle [7, 8]. While it is advantageous in its technological simplicity and maturity to produce FEL pulses with excellent transverse coherence, a typical SASE FEL has rather limited temporal coherence and large shot-to-shot fluctuation, since SASE FEL starts from the electron beam shot noise. In order to narrow the bandwidth beyond what is nominally produced in the standard SASE, several techniques have been developed during the past decades [9–14].

An alternative way to significantly improve the temporal coherence and stability of high-gain FELs is employing external seeding schemes, which generally rely on the longitudinal phase space manipulation techniques for electron beams. In the high-gain harmonic generation (HGHG) scheme [15], an external seed laser pulse is used to interact with the electrons in a short undulator, called modulator, to imprint a sinusoidal energy modulation on the electron beam at the optical wavelength scale. This energy modulation then develops into an associated density modulation after passing through the following small chicane, called the dispersion section (DS). The periodic density modulation contains high-harmonic components of the seed laser frequency, which can be used for generating fully coherent short-wavelength FEL pulses.

The short-wavelength coverage of a single-stage HGHG is limited by the requirement of FEL amplification on the beam energy spread. To increase the frequency multiplication efficiency of the external seeding FEL, many complicated new techniques were developed, e.g., the cascaded HGHG [16], the echo-enabled harmonic generation (EEHG) [17, 18], and the phase-merging enhanced harmonic generation (PEHG) [19, 20]. In the cascaded HGHG scheme, the short-wavelength radiation pulse generated by the intermediate radiator is sent into the downstream HGHG stage and used as the seed laser with the "fresh bunch" technique. However, extending the

This work was partially supported by the National Development and Reform Commission ([2013]2347), National Natural Science Foundation of China (No. 11475250), and the Youth Innovation Promotion Association CAS (2015209).

✉ Zhen-Tang Zhao
zhaozhentang@sinap.ac.cn

[1] Shanghai Institute of Applied Physics, Chinese Academy of Sciences, Shanghai 201800, China

output wavelength to the sub-nanometer region would request cascading three or more stages of HGHG, which would result in a quite complicated setup, with a very long electron bunch for the multiple fresh bunch purpose. Also, there are concerns over the noises accumulated from cascaded stages [21]. The insignificant noise in the seed laser and electron beam may spoil heavily the temporal properties of the generated X-ray FEL due to the harmonic up-conversion processes. It is therefore widely accepted that cascaded HGHG can hardly push the wavelength down to the sub-nanometer region.

An effective way to circumvent the need for multiple stage cascading of external seeding schemes is to increase the harmonic up-conversion efficiency in a single stage, e.g., by employing the EEHG or PEHG techniques. The EEHG scheme adopts two modulator–chicane sections to enhance the coherent micro-bunching at short wavelength with relative small laser-induced energy spread. The modulation mechanism of EEHG was demonstrated at the Next Linear Collider Test Accelerator (NLCTA) [22, 23] and the SDUV-FEL [24]. In a recent experiment, NLCTA demonstrated the generation of VUV radiation at the 75th harmonic of the seed [25], showing distinct advantages of EEHG at high-frequency up-conversion efficiency and paving the way for coherent soft X-ray generation with a single-stage setup. Analyses within the framework of idealized models also indicate the possibility of generating coherent radiation pulse at sub-nanometer wavelengths or even in the hard X-ray regime by combining two-stage cascaded EEHG schemes [26, 27], and the noise amplification problem may be solved by adding a soft X-ray monochromator between the two stages [27]

In this paper, we propose a variant of the cascaded EEHG scheme for the realization of fully coherent hard X-ray generation based on a superconducting linac-driven FEL. A detail design of the monochromator is given. Three-dimensional simulations demonstrate that GW level fully coherent hard X-ray pulses at 0.15 nm can be generated via the proposed technique.

2 Layout of the proposed scheme

A schematic layout of the proposed scheme is shown in Fig. 1. It has two EEHG stages and a soft X-ray monochromatic and fresh beam section. The harmonic up-conversion number for each stage is a few tens. The total harmonic up-conversion number for the two stages is on the order of a few thousand, which means that hard X-rays can be directly generated from a UV commercial laser. Different from the conventional fresh bunch technique that utilizes only one electron bunch, in the proposed scheme, two electron bunches are generated by two drive laser pulses, separated by one RF cycle. The two electron bunches are accelerated and compressed in the adjacent RF cycles in the linac to generate high-brightness double-pulse electron beams (Fig. 1b). The bunch durations can be separately tuned by adjusting the durations of the two drive laser pulses. The proposed scheme is equivalent to having two separate concatenated seeded X-ray FELs. In order to maintain the electron beam quality and suppress the radiation noise in the radiators, an RF kicker is added upstream of the undulator system to provide a transverse deflection [28]. In the first EEHG stage, the head bunch (the longer one) passes through the undulator on axis to reach the saturation regime, generating a coherent soft X-ray pulse with two UV seed lasers, while the tail bunch (the short one) oscillates around the axis to significantly reduce the FEL gain and maintain the beam quality. This kind of “fresh slice” technique has already been demonstrated in recent experiments at the LCLS [29]. The soft X-ray pulse generated from the first stage is filtered through a monochromator and delayed by one RF cycle to seed the tail electron bunch in the second EEHG stage, where the tail electron bunch is put on axis to generate coherent radiation at higher harmonics, and the head electron bunch oscillates around the axis to avoid generating SASE noise in R2.

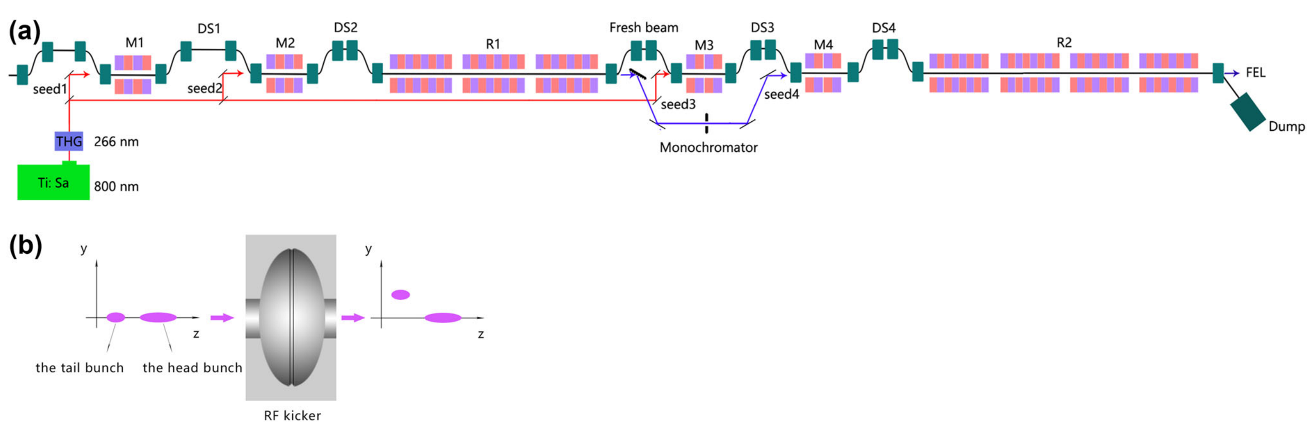

Fig. 1 (Color online) Schematic layout of the proposed scheme for coherent hard X-ray generation: **a** undulator system and **b** RF kicker

The EEHG scheme contains two modulation–chicane sections. The first modulation–chicane section filaments the electron beam in the longitudinal phase space. The second modulation–chicane section then simultaneously bunches each filament, leading to multiple density spikes within each seed wavelength. One practical difficulty of EEHG is using two synchronized seed laser pulses to interact with the same electron beam in the two modulators. For the first-stage EEHG, the two seed lasers pulses can be simply obtained by splitting a single UV laser pulse by using optical methods. However, this becomes extremely complicated and a great challenge for the second stage, due to the lack of materials that are suitable for splitting and reflecting soft X-rays in high efficiency. To mitigate this problem, here we propose using different seed lasers in the second stage. As shown in Fig. 1, the UV seed laser at 266 nm has been split into three branches (Seeds 1–3). Seeds 1 and 2 are injected into the modulators of the first stage, and Seed 3 is injected into the first modulator (M3) of the second stage. The soft X-ray pulse from the first stage works just as the second seed laser of the second stage EEHG.

According to the basic theory of EEHG [17, 18], the output frequency ω_{FEL} is determined by the two seed lasers:

$$\omega_{\mathrm{FEL}} = n\omega_1 + m\omega_2, \tag{1}$$

where ω_1 and ω_2 are the frequencies of the two seed lasers, and n and m are integer numbers. Generally, the bunching factor at ω_{FEL} reach its maximum absolute value when $n = -1$. So, Eq. (1) is written as $\omega_{\mathrm{FEL}} = m\omega_2 - \omega_1$. The m should be large for a large harmonic number, and the output frequency of EEHG is mainly determined by the frequency of the second seed laser.

For the first-stage EEHG, the frequencies of the two seed lasers are equal. The output frequency should be $\omega_{\mathrm{FEL1}} = k_1\omega_1$, where $k_1 = m - 1$ is the harmonic number of the first stage. For the second-stage EEHG, the final output frequency can be written as

$$\omega_{\mathrm{FEL2}} = (k_1k_2 - 1)\omega_1, \tag{2}$$

where k_2 is the harmonic number of the second stage.

3 Design considerations for the monochromator

The monochramator has two functions. It is used for filtering the radiation from the first stage to generate a fully coherent seed for the second stage, and for delaying the radiation pulse by one RF cycle, i.e., about 23 cm for the L-band super conducting accelerator, to make the seed laser overlap with the second electron bunch in the second-stage EEHG. The designed monochromator is shown schematically in Fig. 2.

The grating monochromator has five components: a toroidal varied line space (VLS) grating, two plane mirrors, a spherical mirror, and a slit. The VLS grating disperses and focuses the light tangentially. The dispersed light passes through a slit to select a narrower bandwidth. A removable plane mirror deflects the monochromatic light to the horizon direction, and the light is focused on the entrance of the undulator tangentially and deflected by a cylindrical mirror. Finally, another plane mirror is used to direct the light to the following undulator. The grating monochromator is designed to satisfy the following physical requirements:

1. The power resolution needs to be high enough to generate monochromatic light with sufficient narrow bandwidth;
2. The optical system makes an adequate time delay of the radiation pulse for its overlap with the tail electron bunch;
3. High transition efficiency is required to provide sufficient power to seed the second-stage EEHG; and
4. The whole length of the monochromator should be fit to the undulator system.

Design parameters for the monochromator are given in Table 1. With the parameters, the monochromator resolution is calculated at about 10,000. The incidence and diffraction angles are relatively large, considering that a 25-cm time delay of the optical path should be generated to fit the undulator system. In the grating monochromator design, a VLS grating is used to compensate the image aberration and focus the light tangentially. The gating is toroidal to focus the light vertically and tangentially, hence no need of additional toroidal mirrors in this design. The monochromator is 23.732 m in total length. Its transition efficiency is 3.05% using the Au as the substrate.

To analyze performance of the proposed grating-based monochromator, simulations based on Shadow 3 [30] are carried out at input photon energy of 280 and 280.02 eV. As shown in Fig. 3, the laser pulse of different photon energies after passing through the monochromator can be distinguished clearly. Rationally, the grating monochromator has a power resolution of about 10,000, and it can provide seed pulses with narrow bandwidth.

4 Three-dimensional simulations for the proposed scheme

The performance of an FEL depends crucially on the electron parameters. While analytical calculations only give an estimate of the expected performance, numerical

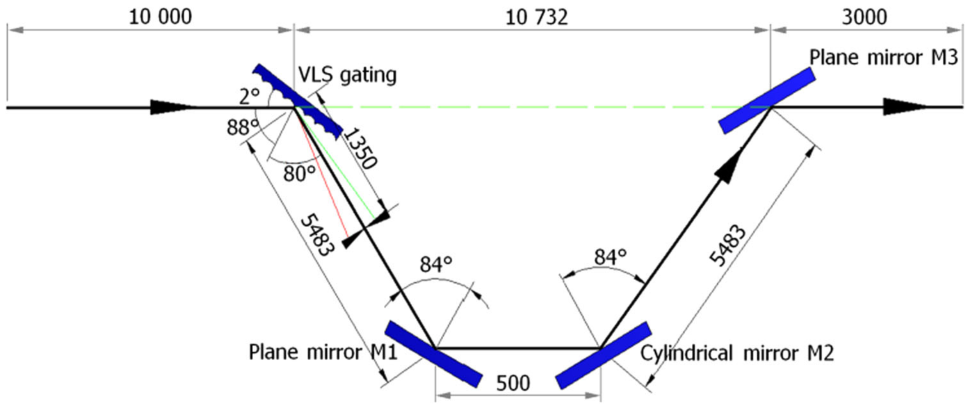

Fig. 2 (Color online) Layout of the monochromator

Table 1 Parameters of the grating monochromator

Parameters	Value @1 keV
Incidence angle	88°
Diffraction angle	80°
D_0 (cm)	32,919
D_1 (cm^2)	489.41
D_2 (cm^3)	16.25
D_3 (cm^4)	0.43665
R_m (m)	190
R_{sag} (cm)	35
f_{obj} (m)	10
f_{image} (m)	1.35
Delay (cm)	25
M2 radius (m)	10.42

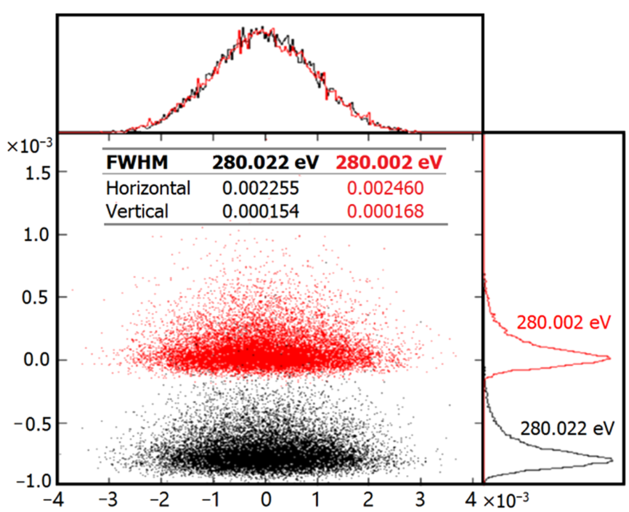

Fig. 3 (Color online) Calculation results on resolution of the monochromator

simulations are necessary to account for various three-dimensional effects and illustrate possible performance of the proposed scheme. Here we perform a three-dimensional tracking of the electron beam, including all components of the soft and hard X-ray undulator beamlines. The optimization of the FEL is conducted using GENESIS [31]. The design specifications used in the simulation are listed in Table 2.

Here we adopt a superconducting linac to drive the FEL. It provides 8 GeV electron beams with peak current of 3 kA and relative slice energy spread of 0.01% at the linac end. As mentioned above, two electron beams of different charges and bunch lengths are generated by the photocathode injector and accelerated in adjacent RF buckets in the linac. The head electron bunch used in the first stage is 300 fs, so as to provide a relative long seed laser for the second stage. The emittance is 1 μmrad for this electron bunch. The tail electron bunch used in the second stage is 80 fs to maintain the low transverse emittance of 0.4 μmrad. The tail electron bunch can be fully covered by the seed pulse from the first stage in the modulator of the second stage, which reduces significantly the timing jitter effects on stability of the final FEL output [27]. An RF kicker to kick the tail electron beam by 10 μrad is adopted, which makes the transverse deviation of the two electron bunches of 100 μm at the entrance of the undulator. The repetition rate of the FEL is 1 kHz, which is mainly limited by the repetition rate of a commercial seed laser. By adopting the optical parametric chirped-pulse amplification (OPCPA) technique, it is possible to produce high-power seed laser pulses with repetition rate up to 100 kHz [32].

There are several challenges in implementing the seeding schemes at extremely high harmonics. In particular, the initial insignificant errors, such as the electron beam shot noise [21] and the seed laser phase error [33], may be amplified by the harmonic up-conversion process and become larger than a much shorter wavelength. To obtain realistic simulation results, we have considered the shot noise in the electron beam and added a random longitudinal phase error of about 1 mrad (rms) into the seed laser pulses. Another challenge is the timing jitter between the relative arrival times of the electron beam and the seed

Table 2 Specifications of the design

Specifications	Soft X-ray beamline (the first stage)	Hard X-ray beamline (the second stage)
Beam energy (GeV)	8	8
Peak current (kA)	3	3
Normalized emittance (μmrad)	1	0.4
Slice energy spread	0.01%	0.01%
Bunch length/fs (FWHM)	300	80
Seed wavelength (nm)	266/266	266/4.33
Seed powers (GW)	2/2	2/1.7
Modulator period (cm)	16/16	16/6
Modulator period numbers	20/10	20/10
Chicane strengths (mm)	8.5/0.145	$4.7 \times 10^{-5}/3.26 \times 10^{-6}$
Radiator period (cm)	6	2
Radiator gap (mm)	11.3	4.7
Radiator length (m)	14	40
Radiation wavelength (nm)	4.43	0.148
Repetition rate (kHz)	1	1

laser, which may cause a large output pulse energy fluctuation due to the electron beam property variations along the longitudinal direction [34, 35]. However, in the proposed scheme, the pulse durations of the seed lasers can be much longer than the electron bunch lengths. In our simulations, the seed laser pulse duration in the 1st stage is 2 ps (FWHM), which is long enough to cover the whole electron bunch and the timing jitter of around 50 fs should not be an issue. The two dispersive chicanes have been tuned to optimize the bunching factor at the 60th harmonic of the seed in the first stage.

Figure 4 shows the FEL gain process in the radiator of the first stage. At the entrance of the radiator, the maximal bunching factor at 4.43 nm is around 10%. This large

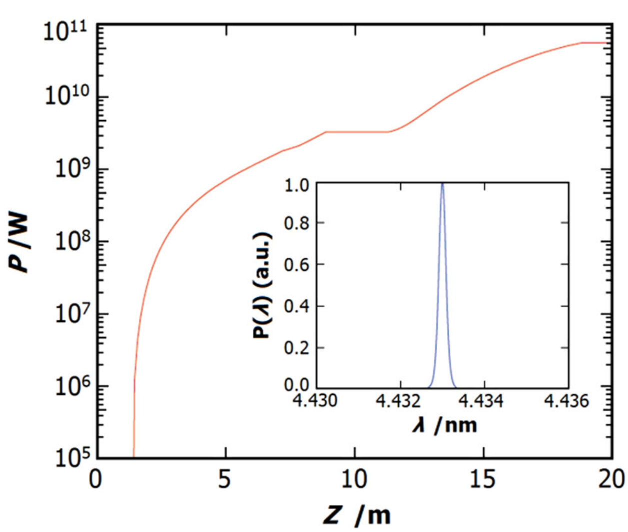

Fig. 4 (Color online) Simulation results for the first-stage EEHG

bunching factor offered by the EEHG is responsible for the initially steep quadratic growth in power in the first undulator segment. Further exponential amplification begins after 5 m, and ultimate saturation is achieved at about 20 m with saturation peak power of over 50 GW. The corresponding spectrum at saturation is shown in the insert plot of Fig. 4. The bandwidth is quite close to the Fourier transform limit. However, the output radiation pulse still contains noisy spikes both in the longitudinal profile and phase, due to the initial shot noise of the electron beam and phase noise of the seed laser, as shown in Fig. 5a. While the spectral noise is insignificant compared to the signal, it will be further amplified by dozens of times and overwhelm the coherent signal in the following EEHG stage.

Since the coherent radiation has a much narrower bandwidth than the noise, we can use the monochromator to filter out most of the noise component and improve the signal-to-noise ratio. In Fig. 2, a grating-based monochromator system is used to purify the radiation spectrum from the first stage. Figure 5b shows the radiation pulse and phase distributions after the monochromator. One finds that the noises are reduced significantly. However, a drawback of the monochromator is that it reduces the radiation pulse energy. For our case, the transfer efficiency of the monochromator is about 3.05%, which means that the power of the radiation pulse will be reduced to about 1.7 GW after passing through the monochromator.

In the second stage, an electron beam with peak current of 3 kA, emittance of 0.4 μmrad, and bunch length of around 80 fs is sent into the EEHG undulator beamline to interact with the monochromatic light beam from the first

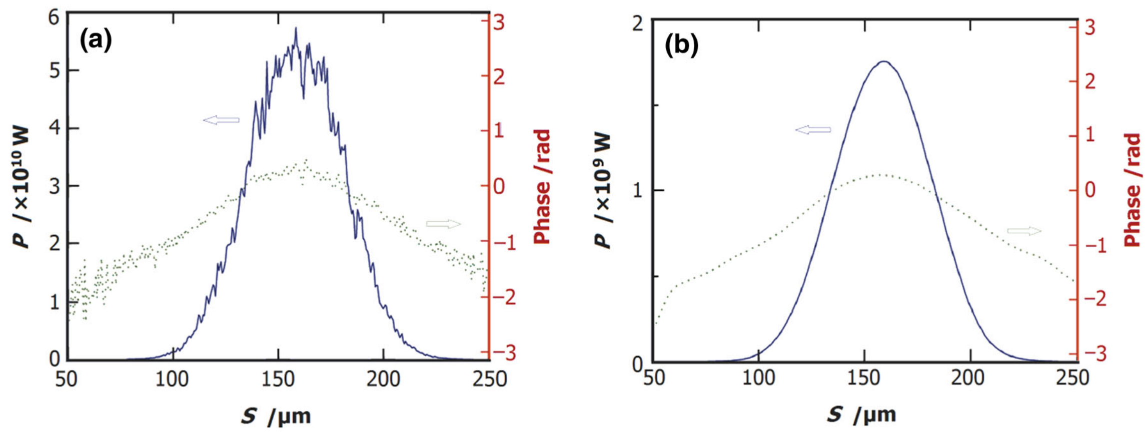

Fig. 5 (Color online) Longitudinal profile (*solid line*) and phase (*dots*) of the FEL radiation pulse before **a** and after **b** the monochromator

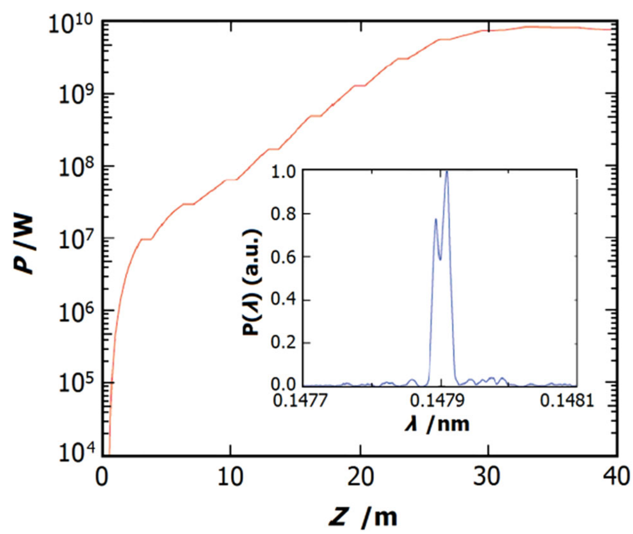

Fig. 6 (Color online) Simulation results for the second-stage EEHG

stage. The radiation pulse from the first stage has a pulse duration of about 300 fs, which is much longer than the electron bunch length in the second stage and thus can relax the timing jitter control requirement. The dispersions are optimized for the bunching factor at the 30th harmonic of Seed 3. In the first modulator, the electron beam interacts with the seed laser pulse at 266 nm. After passing through the first chicane, the electron bunch interacts with Seed 3 at 4.43 nm.

After the modulation process of EEHG, the maximal bunching factor at the 30th harmonic of Seed 3 exceeds 6%. With this large initial bunching factor, Fig. 6 shows the FEL gain process at around 0.148 nm in the final radiator. The FEL output reaches saturation peak power of about 8 GW at around 35 m of the undulator. The bandwidth of the spectrum is about two times of the Fourier transform limit, as shown in the insert of Fig. 6. The simulation results demonstrate that the proposed scheme can generate coherent hard X-ray radiation pulses directly from a UV seed laser source.

5 Conclusion

A two-stage EEHG scheme has been proposed for the superconducting linac-driven FEL to generate coherent hard X-rays. Two electron beam bunches of quite different durations and charges are accelerated by two adjacent RF cycles in the linac to satisfy the different requirements of the two stages. The electron beam used in the first stage is relatively long for generating a long soft X-ray radiation pulse, which can cover the whole electron bunch in the modulator of the second stage and thus significantly improve the FEL output stability. The electron bunch used in the second stage is very short to maintain the low transverse emittance, which is crucial for enhancing the peak power of the final hard X-ray pulse. Simulation results show that, with the state-of-the-art electron gun, accelerator, and undulator technologies, 0.148 nm coherent hard X-ray pulse in peak power of up to 8 GW can be generated directly form 266 nm UV seed lasers. Comparing with some modified schemes based on SASE, the proposed scheme can produce more stable hard X-ray pulses with better temporal coherence. Also, the FEL signal has well-defined timing with respect to the seed laser, thus allowing pump-probe experiment to be performed with much higher temporal resolution. This kind of light source helps to open the door for many challenging experiments which require intense, coherent and ultra-fast hard X-ray pulses.

References

1. W.A. Ackermann, G. Asova, V. Ayvazyan et al., Operation of a free-electron laser from the extreme ultraviolet to the water

window. Nat. Photonics **1**(6), 336–342 (2007). doi:10.1038/nphoton.2007.76
2. P. Emma, R. Akre, J. Arthur et al., First lasing and operation of an ångstrom-wavelength free-electron laser. Nat. Photonics **4**(9), 641–647 (2010). doi:10.1038/nphoton.2010.176
3. T. Ishikawa, H. Aoyagi, T. Asaka et al., A compact X-ray free-electron laser emitting in the sub-angstrom region. Nat. Photonics **6**(8), 540–544 (2012). doi:10.1038/nphoton.2012.141
4. M. Altarelli, R. Brinkmann, M. Chergui et al., The European X-Ray free-electron laser. Technical Design Report. DESY, (2007)
5. R. Ganter, Swiss FEL conceptual design report. PSI, (2011)
6. J.H. Han, H.S. Kang, I.S. Ko, Status of the PAL-XFEL project, in *Proceedings IPAC2012*, New Orleans, LA, USA (2012), pp. 1735–1737
7. A.M. Kondratenko, E.L. Saldin, Generating of coherent radiation by a relativistic electron beam in an undulator. Part. Accel. **10**, 207–216 (1980)
8. R. Bonifacio, C. Pellegrini, L.M. Narducci, Collective instabilities and high-gain regime in a free electron laser. Opt. Commun. **50**(6), 373–378 (1984)
9. J. Feldhaus, E.L. Saldin, J.R. Schneider et al., Possible application of X-ray optical elements for reducing the spectral bandwidth of an X-ray SASE FEL. Opt. Commun. **140**(4), 341–352 (1997). doi:10.1016/S0030-4018(97)00163-6
10. G. Geloni, V. Kocharyan, E. Saldin, Scheme for generation of highly monochromatic X-rays from a baseline XFEL undulator. arXiv preprint arXiv:1003.2548 (2010)
11. J. Amann, W. Berg, V. Blank et al., Demonstration of self-seeding in a hard-X-ray free-electron laser. Nat. Photonics **6**(10), 693–698 (2007). doi:10.1038/nphoton.2012.180
12. D. Xiang, Y. Ding, Z. Huang et al., Purified self-amplified spontaneous emission free-electron lasers with slippage-boosted filtering. Phys. Rev. Spec. Top. Accel. Beams **16**(1), 010703 (2013). doi:10.1103/PhysRevSTAB.16.010703
13. J. Wu, C. Pellegrini, A. Marinelli et al., X-ray spectra and peak power control with ISASE, in *Proceedings of IPAC2013*, 2068–2070, Shanghai, China (2013)
14. B.W. McNeil, N.R. Thompson, D.J. Dunning, Transform-limited X-ray pulse generation from a high-brightness self-amplified spontaneous-emission free-electron laser. Phys. Rev. Lett. **110**(13), 134802 (2013). doi:10.1103/PhysRevLett.110.134802
15. L.H. Yu, Generation of intense UV radiation by subharmonically seeded single-pass free-electron lasers. Phys. Rev. A **44**(8), 5178–5193 (1991). doi:10.1103/PhysRevA.44.5178
16. L.H. Yu, I. Ben-Zvi, High-gain harmonic generation of soft X-rays with the “fresh bunch” technique. Nucl. Instr. Methods Phys. Res. Sect. A **393**(1), 96–99 (1997). doi:10.1016/S0168-9002(97)00435-X
17. G. Stupakov, Using the beam-echo effect for generation of short-wavelength radiation. Phys. Rev. Lett. **102**(7), 074801 (2009). doi:10.1103/PhysRevLett.102.074801
18. D. Xiang, G. Stupakov, Echo-enabled harmonic generation free electron laser. Phys. Rev. Spec. Top. Accel. Beams **12**(3), 030702 (2009). doi:10.1103/PhysRevSTAB.12.030702
19. H. Deng, C. Feng, Using off-resonance laser modulation for beam-energy-spread cooling in generation of short-wavelength radiation. Phys. Rev. Lett. **111**(8), 084801 (2013). doi:10.1103/PhysRevLett.111.084801
20. C. Feng, H. Deng, D. Wang, Z. Zhao, Phase-merging enhanced harmonic generation free-electron laser. New J. Phys. **16**(4), 043021 (2014). doi:10.1088/1367-2630/16/4/043021
21. E.L. Saldin, E.A. Schneidmiller, M.V. Yurkov, Study of a noise degradation of amplification process in a multistage HGHG FEL. Opt. Commun. **202**(1), 169–187 (2002). doi:10.1016/S0030-4018(02)01091-X
22. D. Xiang, E. Colby, M. Dunning et al., Demonstration of the echo-enabled harmonic generation technique for short-wavelength seeded free electron lasers. Phys. Rev. Lett. **105**(11), 114801 (2010). doi:10.1103/PhysRevLett.105.114801
23. D. Xiang, E. Colby, M. Dunning et al., Evidence of high harmonics from echo-enabled harmonic generation for seeding x-ray free electron lasers. Phys. Rev. Lett. **108**(2), 024802 (2012). doi:10.1103/PhysRevLett.108.024802
24. Z. Zhao, D. Wang, J. Chen et al., First lasing of an echo-enabled harmonic generation free-electron laser. Nat. Photonics **6**(6), 360–363 (2012). doi:10.1038/nphoton.2012.105
25. E. Hemsing, M. Dunning, B. Garcia et al., Echo-enabled harmonics up to the 75th order from precisely tailored electron beams. Nat. Photonics **10**(8), 512–515 (2016). doi:10.1038/nphoton.2016.101
26. C. Feng, Z.T. Zhao, Hard X-ray free-electron laser based on echo-enabled staged harmonic generation scheme. Chin. Sci. Bull. **55**(3), 221–227 (2010). doi:10.1007/s11434-010-0002-0
27. Z. Zhao, C. Feng, J. Chen, Z. Wang, Two-beam based two-stage EEHG-FEL for coherent hard X-ray generation. Sci. Bull. **61**(9), 720–727 (2016). doi:10.1007/s11434-016-1060-8
28. C. Emma, Y. Feng, D.C. Nguyen et al., Compact double-bunch X-ray free electron lasers for fresh bunch self-seeding and harmonic lasing. Phys. Rev. Accel. Beams **20**(3), 030701 (2017). doi:10.1103/PhysRevAccelBeams.20.030701
29. A.A. Lutman, T.J. Maxwell, J.P. MacArthur et al., Fresh-slice multicolour X-ray free-electron lasers. Nat. Photonics **10**(11), 745–750 (2016). doi:10.1038/nphoton.2016.201
30. F. Cerrina, C. Welnak, G.J. Chen et al., Shadow 3 Documentation (2011), http://www.esrf.eu/Instrumentation/software/data-analysis/xop2.3
31. S. Reiche, GENESIS: a fully 3D time-dependent FEL simulation code. Nucl. Instr. Methods Phys. Res. Sect. A **429**(1), 243–248 (1999). doi:10.1016/S0168-9002(99)00114-X
32. H. Höppner, A. Hage, T. Tanikawa et al., An optical parametric chirped-pulse amplifier for seeding high repetition rate free-electron lasers. New J. Phys. **17**(5), 053020 (2015). doi:10.1088/1367-2630/17/5/053020
33. D. Ratner, A. Fry, G. Stupakov et al., Laser phase errors in seeded free electron lasers. Phys. Rev. Spec. Top. Accel. Beams **15**(3), 030702 (2012). doi:10.1103/PhysRevSTAB.15.030702
34. E. Allaria, D. Castronovo, P. Cinquegrana et al., Two-stage seeded soft-X-ray free-electron laser. Nat. Photonics **7**(11), 913–918 (2013). doi:10.1038/nphoton.2013.277
35. Z. Wang, C. Feng, Q. Gu et al., Study of the output pulse stability of a cascaded high-gain harmonic generation free-electron laser. Nucl. Instr. Methods Phys. Res. Sect. A **820**, 1–7 (2016). doi:10.1016/j.nima.2016.02.073